



Original article

Novel imidazo[4,5-*b*]pyridine and triaza-benzo[*c*]fluorene derivatives: Synthesis, antiproliferative activity and DNA binding studies

Marijana Hranjec^{a,*}, Borka Lučić^a, Ivana Ratkaj^b, Sandra Kraljević Pavelić^b, Ivo Piantanida^c, Krešimir Pavelić^b, Grace Karminski-Zamola^{a,*}

^a Faculty of Chemical Engineering and Technology, Department of Organic Chemistry, University of Zagreb, Marulićev trg 20, P. O. Box 177, HR-10000 Zagreb, Croatia

^b Department of Biotechnology, University of Rijeka, Trg braće Mažuranića 10, HR-51000 Rijeka, Croatia

^c "Ruder Bošković" Institute, Division of Organic Chemistry and Biochemistry, P. O. Box 180, HR-10002 Zagreb, Croatia

ARTICLE INFO

Article history:

Received 11 January 2011

Received in revised form

17 March 2011

Accepted 30 March 2011

Available online 6 April 2011

Keywords:

Imidazo[4,5-*b*]pyridines
 Triaza-benzo[*c*]fluorenes
 Antiproliferative activity
 Interaction with ct-DNA
 Apoptosis
 Cell cycle

ABSTRACT

In the present paper, we have described the synthesis and biological activity of the novel derivatives of imidazo[4,5-*b*]pyridines and triaza-benzo[*c*]fluorenes (**7–21**, **24–26**, **28–29**). A preponderance of these compounds exerted strong cytostatic effects on the panel of seven human tumour cell lines in a dose-dependent manner. In particular, imidazo[4,5-*b*]pyridines and triaza-benzo[*c*]fluorenes including 2-imidazolyl derivatives showed the most potent antitumour activity. Similarly, triaza-benzo[*c*]fluorenes **18** and **20** induced strong growth inhibition of tested tumour cell lines, and showed low cytotoxicity in normal human fibroblasts. DNA interaction studies of these compounds demonstrated that *N*-methylated **16** and 2-imidazolyl **28** triaza-benzo[*c*]fluorenes bind to DNA in an intercalative mode.

© 2011 Elsevier Masson SAS. All rights reserved.

1. Introduction

Imidazo[4,5-*b*]pyridines represent the major backbone of numerous medical and biochemical agents possessing different chemical and pharmacological features [1,2], which impart them diverse biological properties like anticancer [3,4], antiviral [5–7], antimetabolic [8], anti-inflammatory [9] and tuberculostatic [10] activity. In addition, they can act as antagonists of various biological receptors [11], e.g. angiotensin-II1, platelet activating factor (PAF)2 [12], metabotropic glutamate subtype V3 [13] and AT1 receptor [14]. Importantly, imidazo[4,5-*b*]pyridine is a structural analogue of purine whose derivatives easily interact with large biomolecules such as DNA, RNA or diverse proteins *in vivo*. It is these particular biomolecules that represent the major targets in current drug development strategies aimed at producing next generation therapeutics for untreatable diseases such as cancer [15–19]. DNA plays a central role in life processes, as it stores complete heritage information and mediates protein biosynthesis.

Therefore, understanding the interactions between small organic molecules and DNA might help lay the groundwork for rational development of novel and more selective anticancer agents [20,21].

We have recently reported on the synthesis and biological activity of a series of amidino-substituted heterocyclic benzimidazole, benzimidazo[1,2-*a*]quinoline and diaza-cyclopenta[*c*]fluorene derivatives [22–24]. Biological activity studies comprising cytostatic evaluation, DNA/RNA interaction study and proteomic profiling [24] confirmed the anticancer potential of this class of compounds and suggested further *in vivo* investigation into their possible clinical utility. The same studies also revealed imidazolyl-substituted benzimidazo[1,2-*a*]quinoline to be the most active compound (Fig. 1) with pronounced selectivity towards colon carcinoma cells, which inhibited human topoisomerase II and induced strong G2/M cell cycle arrest indicative of impaired mitotic progression. We also showed that some positively charged analogues of benzimidazo[1,2-*a*]quinolines and diaza-cyclopenta[*c*]fluorenes intercalate into ds DNA or RNA, which might account for their accentuated antiproliferative effect [22,23].

Prompted by the findings from the above mentioned studies, we set out to explore and synthesize novel imidazo[4,5-*b*]pyridine and triaza-benzo[*c*]fluorene derivatives with substituents on different positions of the heterocyclic rings (Fig. 2). Cyclic imidazo[4,5-*b*]

* Corresponding authors. Tel.: +385 14597245; fax: +385 14597250.

E-mail addresses: mhranjec@fkit.hr (M. Hranjec), gzamola@fkit.hr (G. Karminski-Zamola).

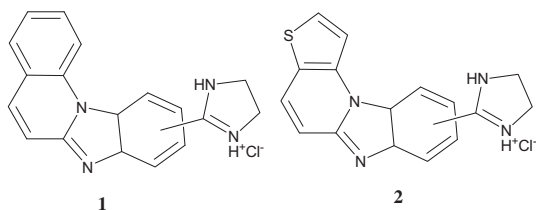


Fig. 1. Structures of previously prepared 2-imidazolyl substituted benzimidazo[1,2-*a*]quinoline **1** and diaza-cyclopenta[*c*]fluorene **2**.

pyridine derivatives related to triaza-benzo[*c*]fluorenes were prepared photochemically by the dehydrocyclization reaction or by the thermal cyclization reaction. Majority of newly synthesized compounds were tested for their antiproliferative activity on the panel of seven human tumour cell lines. Possible antiproliferative mechanisms and/or targets were studied in details for compounds **18** and **28**, while DNA-binding studies were performed for compounds **16**, **18** and **28**.

2. Results and discussion

2.1. Chemistry

Prepared compounds (Fig. 2) were synthesized according to the procedures shown in Schemes 1, 2 and 3 by the conventional methods of organic synthesis for the preparation of similar heterocyclic compounds [25,26]. Starting from the *E*-3-phenyl-substituted acrylic acids **1–4** (Scheme 1), via the cyclocondensation reaction between the corresponding 2,3-diaminopyridines **5–6** and polyphosphoric acid (PPA), *E*-2-styryl-imidazo[4,5-*b*]pyridines **7–11** were prepared. Their cyclic derivatives, namely triaza-benzo[*c*]fluorenes **12–15**, were prepared by the thermal reaction using sulfolane for dehydrohalogenation cyclization at 280 °C as a mixture of two inseparable regioisomers. Unsubstituted derivative **12** was prepared by the photochemical dehydrocyclization reaction from ethanolic solution of derivative **7**. *N*-methylated derivatives **16–17** were prepared from derivatives **12** and **13** using lower yields of methyl iodide, whereas methylation of triaza-benzo[*c*]derivatives **14–15** failed.

Amino-substituted triaza-benzo[*c*]derivatives **18–19** were prepared according to Scheme 2 by the reduction reaction with

$\text{SnCl}_2 \times 2\text{H}_2\text{O}$ from nitro-substituted precursors **16–17** in very good yields. Hydrochloride salts of the above mentioned amino derivatives **20–21** were prepared by protonation with $\text{HCl}_{(g)}$ to ensure better solubility.

Cyano-substituted *E*-2-styryl-imidazo[4,5-*b*]pyridines **24–25** were prepared in very good yields by the condensation reaction between the corresponding 2-methylimidazo[4,5-*b*]pyridines **22–23** and *p*-cyanobenzaldehyde in a sealed tube at 180 °C using previously described method [27]. Cyano-substituted triaza-benzo[*c*]fluorenes **26–27** were prepared photochemically by subjecting ethanolic solution of compounds **24–25** to irradiation with high-pressure mercury lamp followed by UV/Vis spectroscopy. 2-imidazolyl-substituted triaza-benzo[*c*]fluorenes **28–29** were prepared as hydrochloride salts by the Pinner reaction for amidine synthesis [28,29].

All structures of novel *E*-2-styryl-imidazo[4,5-*b*]pyridine derivatives **7–11** and **24–25**, and derivatives of triaza-benzo[*c*]fluorenes **12–21** and **26–29** were determined by the NMR analysis based on the analysis of H–H coupling constants as well as chemical shifts. In ^1H NMR spectra of *E*-2-styryl-imidazo[4,5-*b*]pyridine derivatives **7–11** and **24–25**, besides all other aromatic protons, two doublets for *trans*-ethylenic protons with coupling constants of ~16.5 Hz can be observed, as well as singlet of the NH group of imidazo[4,5-*b*]pyridine ring around 12 ppm. The cyclization reaction producing “fused” triaza-benzo[*c*]fluorenes caused a downfield shift of the most aromatic protons as well as disappearance of the NH group at the imidazo[4,5-*b*]pyridine ring, thus confirming the cyclic structure formation. In ^1H NMR spectra of all synthesized triaza-benzo[*c*]fluorenes, doublets for two protons on fluorene ring with coupling constants of ~9.5 Hz can be observed.

2.2. Spectroscopic properties of compounds **16**, **18** and **28**

Since DNA binding studies of compounds **16**, **18** and **28** require application of spectrophotometric methods; their aqueous buffered solutions (proven to be stable over prolonged periods of time) were characterized by electronic absorption (UV/Vis) and fluorescence emission spectroscopy (Table 1). The absorbances of buffered aqueous solutions of an each compound were proportional to their concentrations up to $c = 2.0 \times 10^{-5} \text{ mol dm}^{-3}$, changes in the UV/Vis spectra upon the temperature increase up to 98 °C were negligible, and UV/Vis spectra reproducibility after

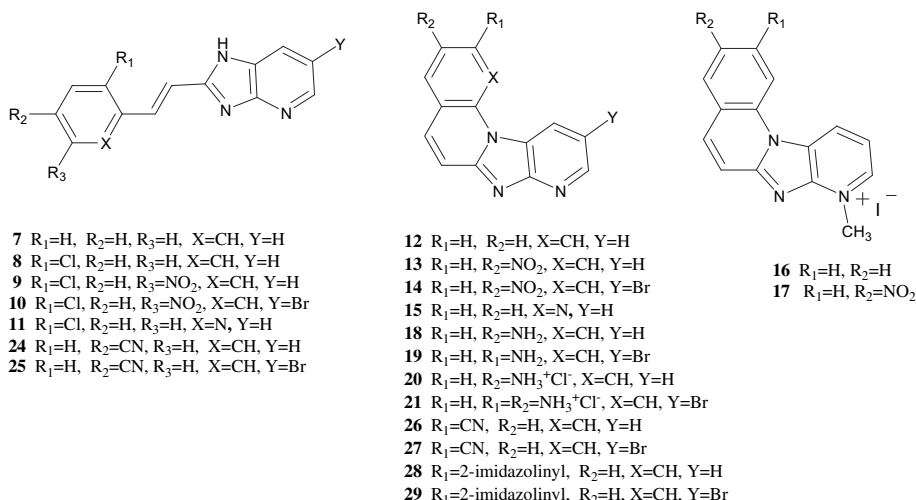
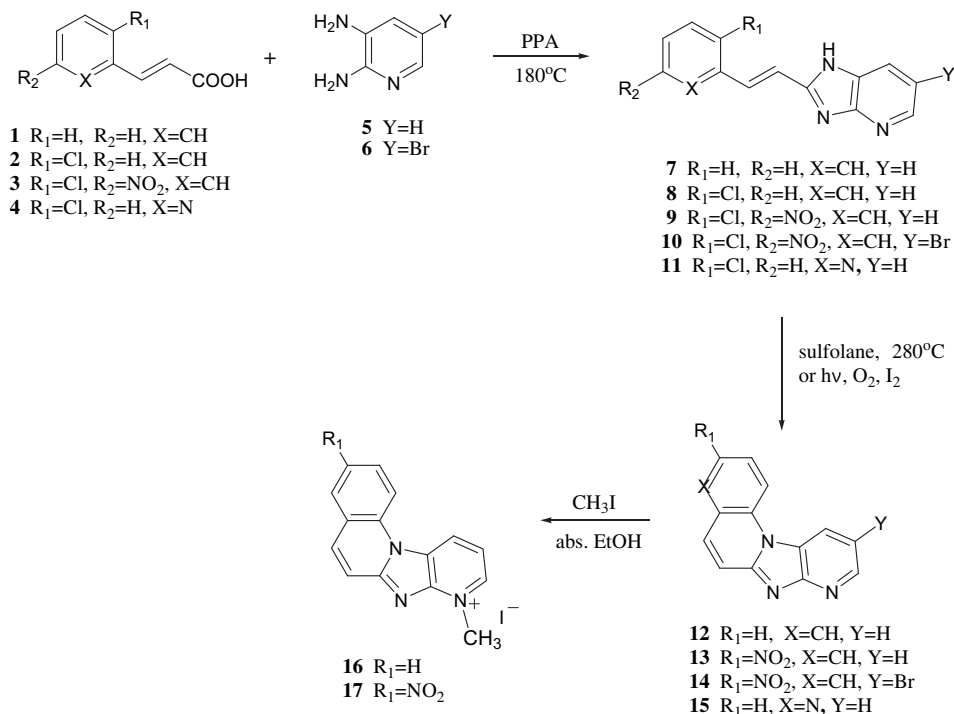


Fig. 2. *E*-2-styryl substituted derivatives of imidazo[4,5-*b*]pyridines **7–11** and **24–25** and derivatives of triaza-benzo[*c*]fluorenes **12–21** and **26–29**.



Scheme 1. Synthesis of *E*-2-styryl substituted imidazo[4,5-*b*]pyridines **7–11** and derivatives of triaza-benzo[*c*]fluorenes **12–17**.

cooling down to 25 °C was excellent. Obtained results indicate that compounds **16**, **18** and **28** do not aggregate by intermolecular stacking under applied experimental conditions (Fig. SM1). Compounds **16**, **18** and **28** exhibited strong fluorescence emission with maximum at 386–519 nm. Fluorescence emissions of **16**, **18** and **28** were proportional to their concentration in the range from 3×10^{-8} mol dm⁻³ to 4×10^{-7} mol dm⁻³, and their excitation spectra were in concordance with the corresponding absorption spectra. Absorption maxima, corresponding molar extinction coefficients (ϵ) and fluorescence emission maxima are presented in Table 1.

2.3. Interaction study for compounds **16**, **18** and **28** with ct-DNA in an aqueous medium

2.3.1. UV/Vis spectrophotometric titrations

Addition of calf-thymus DNA (ct-DNA) resulted in bathochromic and hypochromic effects of UV/Vis spectra of studied compounds. For compounds **16** and **28** (Fig. SM2), significant deviations from the isosbestic points were observed pointing to the coexistence of at least two different types of complexes. The UV/Vis spectra obtained for compounds **16**, **18** and **28** exhibited strong hypochromic changes upon titration with ct-DNA as follows:

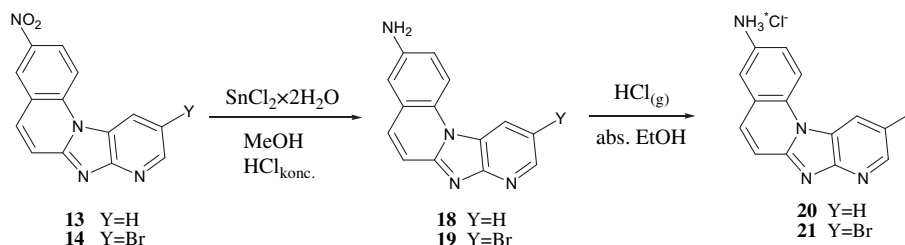
H(**16**) = 28% (327 nm), 37% (342 nm), 38% (360 nm); H(**18**) = 26% (330 nm), 18% (343 nm); and H(**28**) = 45% (347 nm), 35% (364 nm).

2.3.2. Fluorimetric titrations

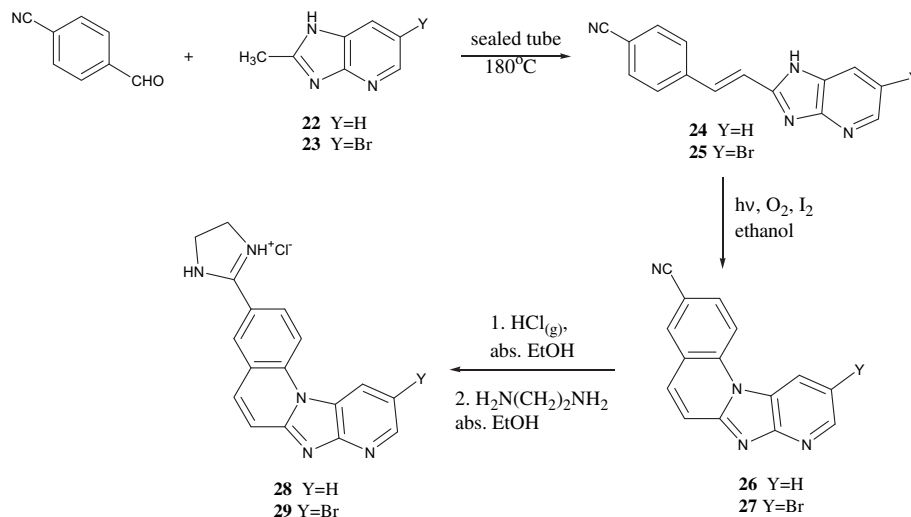
Experimental conditions in UV/Vis titrations resulting in mixed binding modes at high compound/DNA ratios ($r > 0.2$) were circumvented by taking advantage of strong fluorescence of aqueous solutions of compounds **16**, **18** and **28**, which allowed for fluorimetric titrations at lower compound concentrations and collection of many data points at high ct-DNA over compound excess ($r < 0.1$). Addition of ct-DNA completely quenched fluorescence of **28** (Fig. 3A), and strongly quenched fluorescence of **16** (Fig. SM3A) at variance to fluorescence of **18**, whose emission was only negligibly changed.

UV/Vis (**18** and **28**) and fluorimetric (**16** and **28**) titration data were processed by using Scatchard equation [30] giving rise to log K_s values (Table 2).

Comparison of K_s values presented in Table 2 revealed higher affinity of compounds **16** and **28** towards ct-DNA in comparison to free amine analogue **18**. Furthermore, cumulative binding affinity of compound **28** observed in UV/Vis titrations did not yield significantly different K_s value in comparison to the results of fluorimetric titration. Thus, somewhat higher value of ratio n



Scheme 2. Synthesis of amino substituted triaza-benzo[*c*]derivatives **18–21**.



Scheme 3. Synthesis of cyano substituted *E*-2-styryl-imidazo[4,5-*b*]pyridines **24–25**, cyano substituted triaza-benzo[*c*]fluorenes **26–27** and 2-imidazolynyl substituted triaza-benzo[*c*]fluorenes **28–29**.

obtained for UV/Vis titrations can be attributed to agglomeration of an excess of **28** molecules along DNA at conditions at which all dominant binding sites are already occupied ($[\mathbf{28}]/[\text{ct-DNA}] > 0.3$).

2.3.3. CD spectrophotometric titrations

Non-covalent interactions at 25 °C were commonly studied through the assessment of spectroscopic properties of the compound upon polynucleotides addition. We have, however, chosen CD spectroscopy as a highly sensitive method for monitoring conformational changes in the secondary structure of polynucleotides as to investigate the changes in polynucleotide properties induced by small molecule binding [31]. Addition of compound **28** resulted in increase of ct-DNA CD band at 275 nm, as well as in an appearance of weak, negative induced CD band (ICD) at 337 nm (Fig. 4A). Observed weak negative ICD band for compound **28** appeared at UV maximum, which is indicative of intercalation into ct-DNA, whereby longer axis of **28**-hetero-aromatic system is coplanar with the longer axis of adjacent DNA base pairs [32]. Furthermore, compound **28** has another UV maximum with a shoulder at 273 nm (see Fig. SM1 – UV/Vis spectra of free compounds), which similarly to some hetero-aromatic systems might be attributed to transitions along shorter axis of a molecule [33]. Thus, upon intercalation of compound **28** into ct-DNA, such shorter axis should be perpendicular to longer axis of adjacent DNA base pairs, and should subsequently yield weak positive ICD effect noticed as a small increase of CD band at

275 nm. Non-linear dependence of intensity changes at both 275 nm and 337 nm on ratio $r_{[\mathbf{28}]/[\text{ct-DNA}]}$ (Fig. 4B) suggested saturation of dominant binding sites along DNA at ratio $r = 0.3$, which greatly correlates with Scatchard ratio n calculated from fluorimetric titration.

A titration of ct-DNA with compound **16** yielded similar changes to those noticed for compound **28** characterized by a weak negative ICD band at 325 nm. At excess of compound **16** over ct-DNA ($r > 0.3$), an additional weak positive ICD band at 350–400 nm appears, which might be ascribed to non-specific agglomeration of the compound along DNA.

A titration of ct-DNA with compound **18** revealed a small increase of CD band at 275 nm and an absence of ICD band at >300 nm implying small changes in the helical structure of DNA upon compound **18** binding. An absence of ICD band might point to the non-homogenous orientation of bound molecules of compound **18** relative to the DNA helical axis.

2.3.4. Thermal denaturation experiments

In thermal denaturation experiments, addition of cyclic derivatives **16** and **28** moderately stabilized ct-DNA, with a significant non-linear dependence of ΔT_m values on the ratio r (Table 3). Addition of compound **18** negligibly stabilized ct-DNA against thermal denaturation ($\Delta T_m = 1\text{--}2$ °C for ratio $r_{[\mathbf{28}]/[\text{ct-DNA}]} = 0.2\text{--}0.3$).

2.4. Discussion of interactions of **16**, **18** and **28** with ct-DNA

Intercalation of **16** and **28** as a dominant binding mode was demonstrated by a weak negative ICD band > 300 nm, significant bathochromic and hypsochromic changes in UV/Vis titration, thermal stabilization of DNA as well as by values of $K_s > 10^5 \text{ M}^{-1}$. At excess of **16** or **28** over intercalative binding sites, non-specific agglomeration along DNA double helix occurs. Surprisingly, free amine analogue **18** induced significantly lower changes in UV/Vis and fluorescence spectrum upon addition of ct-DNA in comparison to **16** and **28**; stabilization of ct-DNA against thermal denaturation and appearance of the ICD band >300 nm did not occur. Moreover, affinity was significantly lower in comparison to **28** pointing to a much weaker, non-intercalative binding mode, which is most likely a heterogeneous agglomeration of randomly oriented molecules of compound **18** within the DNA minor groove that causes a lack of positive ICD effect.

Table 1

Electronic absorption maxima, molar extinction coefficients and fluorescence emission maxima of studied compounds.^a

Comp.	Absorption maxima		Fluorescence emission
	$\lambda_{\text{max}}/\text{nm}$	$\epsilon \times 10^3/\text{dm}^3 \text{ mol}^{-1} \text{ cm}^{-1}$	$\lambda_{\text{max}}/\text{nm}$
16	360	18.67	386
	343	22.72	406
	327	20.66	
	226	50.86	
18	342	31.60	519
	329	30.67	
	262	61.91	
28	348	9.87	466
	239	26.16	

^a Sodium cacodylate buffer $I = 0.05 \text{ mol dm}^{-3}$, pH = 7.

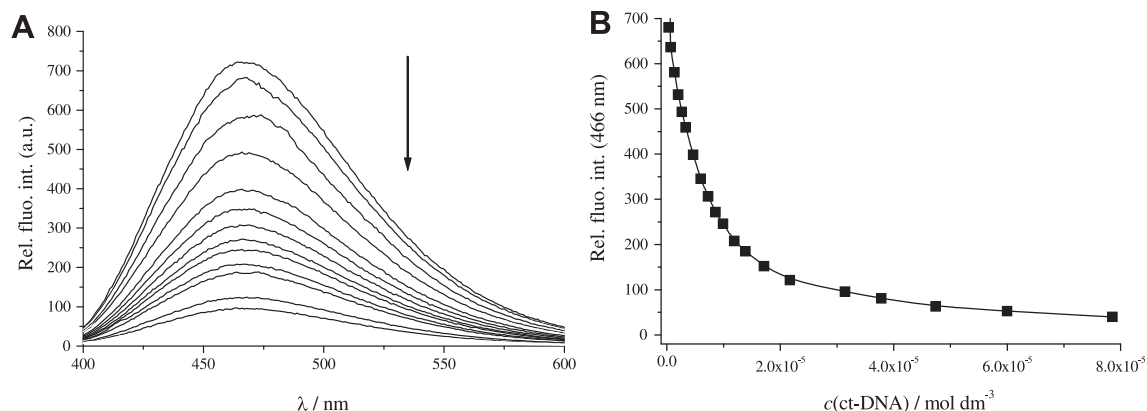


Fig. 3. A) Changes in fluorescence spectrum of **28** ($c = 5.8 \times 10^{-7} \text{ mol dm}^{-3}$) upon titration with ct-DNA ($c = 2.00 \times 10^{-2} \text{ mol dm}^{-3}$); B) Dependence of **28** emission at $\lambda = 466 \text{ nm}$ on $c(\text{ct-DNA})$; All experiments were carried out at $\text{pH} = 7.0$, (buffer sodium cacodylate $I = 0.05 \text{ mol dm}^{-3}$).

2.5. Biological results and discussion of antiproliferative activity

Novel imidazo[4,5-*b*]pyridine and triaza-benzo[*c*]fluorene derivatives (**1–21**, **24–26** and **28–29**) were evaluated for their antiproliferative activity *in vitro* using the panel of seven human cell lines derived from different tumour types including HeLa (cervical carcinoma), SW620 (colorectal adenocarcinoma, metastatic), MiaPaCa-2 (pancreatic carcinoma), MCF-7 (breast epithelial adenocarcinoma, metastatic), HEp-2 (epidermoid carcinoma, larynx) and SK-BR-3 (breast adenocarcinoma, metastatic) as well as normal diploid human fibroblasts (WI38). Their cytostatic effect was compared against that of two commonly used chemotherapeutics, namely cisplatin and 5-fluorouracil (5-FU). Obtained results are summarized and presented in Table 4, and are in line with our previously published data showing strong antitumour activity of several heterocyclic benzimidazole, benzimidazo[1,2-*a*]quinoline and diaza-cyclopenta[*c*]fluorene derivatives [22,23,26].

With the exception of compounds **11** and **15** that exerted none or modest antiproliferative activity, the majority of tested compounds demonstrated strong cytostatic effect on all tested cell lines in a dose-dependent manner (Fig. SM4), especially at micromolar concentrations ranging from 1 to 10 μM for *E*-2-styryl substituted derivatives of imidazo[4,5-*b*]pyridines **7**, **8**, **10** and **25**, and for triaza-benzo[*c*]fluorenes **16**, **18**, **19**, **20**, **28** and **29** (Table 4).

Compounds **16**, **18** and **20** showed selective effect on SK-BR-3 cells. Besides the latter cell line, compound **16** specifically inhibited the growth of MCF-7 and HeLa cells as well. Among triaza-benzo[*c*]fluorenes, the strongest non-specific effect on all cell lines at micromolar concentrations (0.1–10 μM) was detected for triaza-benzo[*c*]fluorenes **28** and **29** bearing the 2-imidazolyl

Table 2

Binding constants ($\log K_s$), ratios $n = ([\text{bound compound}]/[\text{ct-DNA}])$ calculated from fluorimetric and UV/Vis titrations of **16**, **18** and **28** with ct-DNA at $\text{pH} = 7$ (buffer sodium cacodylate, $I = 0.05 \text{ mol dm}^{-3}$).^a

Compound	Fluorescence		UV/Vis	
	$\log K_s$	n	$\log K_s$	n
28	5.9	0.28	5.4 ^c	0.44 ^c
18	^b	^b	4.6	0.24
16	4.9	0.20	–	–

^a Titration data were processed using the Scatchard equation, accuracy of obtained $n \pm 10$ –30%, consequently $\log K_s$ values vary in the same order of magnitude.

^b Too small spectroscopic changes or accurate calculation.

^c Cumulative affinity of **28** since more different complexes are simultaneously present (as shown by deviation of isosbestic points on Fig. 4).

moiety, which probably adds up to their cytotoxicity (IC_{50} values for **28** and **29** were in the same range as those for cisplatin and 5-FU) (Fig. 1). Importantly, compounds **18** and **20** showed lower toxicity in normal human fibroblasts than other biologically active newly synthesized compounds, cisplatin and 5-FU (Table 4). Interestingly, both 4-pyridyl substituted compounds **11** and **15** showed the poorest antiproliferative activity among all tested compounds.

Marked antitumour activities of compounds **18** and **28** have led us to investigate their mechanism of action in more details, especially when having in mind that compound **18** was highly selective for SK-BR-3 cells with low cytotoxicity in normal human fibroblasts, and compound **28** was highly selective for two metastatic cell lines, namely breast adenocarcinoma (SK-BR-3) and colorectal adenocarcinoma (SW620), which are known for their resistance to common chemotherapeutics.

2.6. Cell cycle perturbations and apoptosis induction

The results of the flow cytometric analysis revealed strong perturbations in the cell cycle of MiaPaCa-2 and SW620 cells induced upon treatment with compound **28** (Table 5). Antiproliferative effect of compound **28** on MiaPaCa-2 cells could be associated with S-phase arrest at all tested concentrations accompanied by the rise in the sub-G1 population at 5 μM after 24- and 48-h treatments. Accordingly, an increase in the S-phase arrested cell population by 22.1% and 22.3% after 24- and 48-h exposure, respectively, concurred with the apparent decline in G1-phase cells. Impairment of cell cycle progression in SW620 cells treated with compound **28** for 24 h was characterised by a rise in the G1 cell population by 36.2% accompanied with a decrease in S-phase cells by 15.4%. Prolonged exposure time (48 h) triggered completely opposite effect, namely an increase of 3.6% in S-phase cells with a concomitant reduction in the G1 cell population. Treatment of SW620 cells with compound **28** with the highest tested concentrations (10 μM) for 48 h brought forth different cell cycle distribution pattern marked by G-phase arrest and S-phase cell population up to 30% (Table 5). Growth inhibitory effect of compound **18** on SK-BR-3 cells might be linked with substantial rise in sub-G1 phase up to 11.2% (24 h treatment) and the S-phase arrest upon 48-h treatment, when reduction in the G2/M phase cell population was detected as well (Table 6).

Morphological appearance of MiaPaCa-2, SW620 and SK-BR-3 cells treated with compounds **28** and **18** was also examined (Figs. 5, 6 and 7). Changes in cell morphology typical of apoptosis,

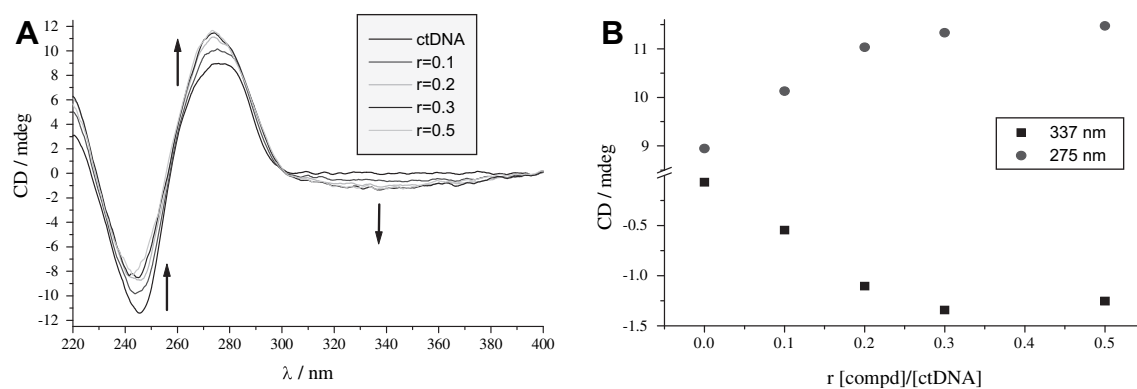


Fig. 4. A) Changes in CD spectrum of ct-DNA ($c = 1.0 \times 10^{-5} \text{ mol dm}^{-3}$) upon titration with **28**; B) Dependence of CD band of ct-DNA ($\lambda_{\text{max}} = 274 \text{ nm}$) and ICD band of **28** ($\lambda_{\text{max}} = 337 \text{ nm}$) on $r = [\mathbf{28}]/[\text{ct-DNA}]$, at pH = 7, sodium cacodylate buffer, $I = 0.05 \text{ mol dm}^{-3}$.

such as cell shrinkage and chromatin condensation, were detected in SW620 cells treated with compound **28** (5 and 10 μM) as well as in MiaPaCa-2 cells treated with the highest tested concentration (10 μM) of the same compound. These results are in good agreement with the findings of the flow cytometric analysis demonstrating significant increase in the sub-G1 cell population indicative of apoptotic cell death (Table 5). When treated with lower concentrations of compound **28**, the majority of MiaPaCa-2 cells became visibly enlarged, which corresponds to S-phase arrest revealed by the cell cycle analysis. In addition, exposure of SW620 cells to the lowest tested concentration (1 μM) of this compound resulted in cell morphology reminiscent of that found in cells undergoing cell cycle arrest, which correlates with S-phase arrest detected after 24 and 48 h of treatment, respectively, by flow cytometric analysis. Based on these results, one can conclude that compound **28** triggered apoptosis in MiaPaCa-2 and SW620 cells in a dose-dependent manner, which could be ascribed to its ability to intercalate into ds DNA. On the contrary, SK-BR-3 cells showed rather low percentage of visible apoptotic cells. When treated with compound **18**, these cells became enlarged, possibly due to S-phase arrest confirmed by flow cytometry. Weaker DNA-damaging effect of compound **18** illustrated by an absence of apoptotic features might stem from the lack of its intercalative properties. It is most likely that compound's **18** molecules form agglomerates within DNA minor groove and/or interact with other biologically active molecules involved in DNA synthesis (e.g. enzymes of the replication machinery) thus preventing the cells from completing the replication of their genetic material as a prerequisite for successful cellular division.

3. Conclusions

The present paper deals with the synthesis of novel derivatives related to imidazo[4,5-*b*]pyridines (**7–11** and **24–25**) and triaza-benzo[*c*]fluorenes (**12–21** and **26–29**). We have previously

shown that these groups of compounds exert strong anti-proliferative effect on all tested cell lines in a dose-dependent manner, which makes them promising lead compounds for further pre-clinical investigation. The strongest non-specific antiproliferative effect was observed for triaza-benzo[*c*]fluorenes **28** and **29** bearing the 2-imidazolynyl moiety, which probably adds up to their high cytotoxicity. Contrary to these two compounds, triaza-benzo[*c*]fluorenes **18** and **20** showed lower toxicity in normal human fibroblasts when compared with cisplatin and 5-FU used as control chemotherapeutics. Induction of apoptosis was detected in SW620 and MiaPaCa-2 cells treated with compound **28** at higher concentrations, while lower concentrations gave rise to S-phase arrest. Apoptosis induction by this compound was dose-dependent and was directly associated with its ability to intercalate into ds DNA, as corroborated by the spectrophotometric DNA interaction study showing *N*-methyl-substituted compounds **16** and 2-imidazolynyl-substituted **28** triaza-benzo[*c*]derivatives to intercalate into ds DNA. Free amine analogue **18** binds to DNA by the non-intercalative binding mode, which might be partially responsible for observed lower cytotoxicity in SK-BR-3 cells and control fibroblasts. It is most likely that compound's **18** molecules form agglomerates within DNA minor groove and/or interact with other biologically active molecules involved in DNA synthesis, such as DNA replication enzymes, leading to an arrest of DNA synthesis.

4. Experimental

4.1. Chemistry

4.1.1. General methods

Melting points were determined by Koffler hot-stage microscope, and were uncorrected. IR spectra were recorded on FTIR-ATR and Perkin–Elmer Spectrum 1 spectrophotometers. ^1H and ^{13}C NMR spectra were recorded on Varian Gemini 300, Bruker Avance DPX 300 and Bruker Avance DRX 500 spectrometers using TMS as an internal standard in $\text{DMSO-}d_6$. Elemental analyses for carbon, hydrogen and nitrogen were performed on Perkin–Elmer 2400 elemental analyzer and Perkin–Elmer, Series II, CHNS Analyzer 2400. Where analyses are indicated only as symbols of elements, analytical results obtained were within 0.4% of the theoretical value. In preparative photochemical experiments, the irradiation was performed at room temperature with water-cooled immersion well with “Origin Hanau” 400-W high-pressure mercury arc lamp using Pyrex glass as a cut-off filter of wavelengths below 280 nm. All compounds were routinely checked by TLC with Merck silica gel 60F-254 glass plates.

Table 3

ΔT_m values^a ($^{\circ}\text{C}$) of ct-DNA upon addition of different ratios b_r of **16**, **18** and **28** at pH = 7.0 (buffer sodium cacodylate, $I = 0.05 \text{ mol dm}^{-3}$).

b_r	16	18	28
0.1	1.60	0.70	2.70
0.2	2.60	1.40	5.10
0.3	4.25	0.20	6.40
0.5	6.10	1.30	8.40

^a Error in ΔT_m : $\pm 0.5 \text{ }^{\circ}\text{C}$.

^b $r = [\text{compound}]/[\text{polynucleotide}]$.

Table 4
IC₅₀ values of compounds **7–21**, **24–29** (μM) and control compounds cisplatin and 5-fluorouracil (5-FU).

Substance No.	Cell lines						
	HeLa	MCF-7	HEp-2	SK-BR-3	SW620	MiaPaCa-2	WI38
7	2.22	7.57	3.89	2.06	4.64	4.39	3.87
8	31.62	25.56	29.29	5.79	50.94	59.09	>100
9	45.06	53.65	49.36	1.80	51.99	38.79	61.60
10	3.68	8.81	0.91	59.92	7.99	30.59	6.48
11	>100	>100	>100	53.14	>100	>100	>100
12	14.32	75.45	52.28	83.52	78.28	80.52	47.41
13	52.77	>100	>100	42.74	>100	>100	75.71
14	13.38	>100	31.09	8.11	61.25	63.53	>100
15	>100	>100	>100	>100	>100	>100	>100
16	7.52	7.56	13.19	3.51	14.75	8.56	6.27
17	11.43	>100	31.52	33.57	26.69	>100	>100
18	43.36	72.38	39.24	2.94	34.77	48.18	>100
19	30.91	61.70	14.09	7.76	38.65	33.04	85.37
20	27.16	55.96	26.69	3.64	25.91	43.42	>100
21	37.73	67.30	21.55	7.56	40.69	40.32	85.09
24	47.06	12.89	84.91	86.56	>100	>100	>100
25	2.88	7.82	5.69	4.31	7.11	8.17	6.76
26	39.46	>100	47.28	67.72	>100	>100	51.47
28	0.41	6.54	0.27	2.20	0.64	0.74	1.768
29	1.10	8.43	4.01	5.52	3.67	4.74	3.71
Cisplatin	0.35	12.61	2.41	14.23	4.01	3.52	0.22
5-FU	10.31	42.01	>100	38.25	3.38	11.45	18.5

^a IC₅₀; 50% inhibitory concentration, or compound concentration required to inhibit tumour cell proliferation by 50%.

4.1.2. General method for the synthesis of triaza-benzo[*c*]fluorene derivatives (**13–15**)

E-2-styryl-1*H*-imidazo[4,5-*b*]pyridine derivatives **7–11** were dissolved in 2–3 ml of sulfolane, and reaction mixture was heated for ½–2 h at 280 °C. The cooled mixture was poured into water (25 ml) and the resulting product was filtered off and recrystallized from ethanol to obtain triaza-benzo[*c*]fluorenes **13–15**.

4.1.2.1. 3-Nitro-7,8,11*b*(11)-triazabeno[*c*]fluorene **13.** Compound **13** was prepared using the above described method from compound **9** (0.50 g, 1.16 mmol) in sulfolane (1.5 ml) after 45 min to obtain yellow powder (0.18 g, 57%). mp > 270 °C; UV (EtOH) λ_{max}/nm = 302, 335, 351, 369; IR (diamond): ν/cm⁻¹ = 3056, 1632, 1616, 1598, 1529; ¹H NMR (DMSO-*d*₆, 600 MHz): a) 9.93 (d, 1H, *J* = 9.3 Hz, H_{arom}), 9.03 (d, 1H, *J* = 2.3 Hz, H_{arom}), 8.40 (dd, 1H, *J*₁ = 8.1 Hz, *J*₂ = 1.3 Hz, H_{arom}), 8.23

(d, 1H, *J* = 9.6 Hz, H_{fluorene}), 7.82 (d, 1H, *J* = 9.6 Hz, H_{fluorene}), 7.66 (Abq, 1H, *J*₁ = 8.12 Hz, *J*₂ = 4.7 Hz, H_{arom}); b) 9.13 (d, 1H, *J* = 8.3 Hz, H_{arom}), 9.08 (d, 1H, *J* = 2.5 Hz, H_{arom}), 8.95 (d, 1H, *J* = 9.3 Hz, H_{arom}), 8.76 (d, 1H, *J* = 4.6 Hz, H_{arom}), 8.54 (dd, 1H, *J*₁ = 9.2 Hz, *J*₂ = 2.5 Hz, H_{arom}), 8.28 (d, 1H, *J* = 9.7 Hz, H_{fluorene}), 7.89 (d, 1H, *J* = 9.6 Hz, H_{arom}), 7.58 (ABq, 1H, *J*₁ = 8.3 Hz, *J*₂ = 4.7 Hz, H_{arom}); ¹³C NMR (DMSO-*d*₆, 150 MHz): 164.1, 163.2, 156.3, 149.6, 144.2, 143.9, 143.1, 142.9, 142.3, 138.7, 133.1, 128.7, 128.0, 127.0, 126.0, 125.0, 123.6, 123.2, 124.9, 124.0, 123.5, 123.4, 119.6, 118.7, 118.3, 117.6, 116.9, 115.9; Anal. (C₁₄H₈N₄O₂) Calcd.: C, 63.7; H, 3.0; N, 21.0; Found: C, 63.9; H, 2.8; N, 21.2.

4.1.2.2. Bromo-3-nitro-7,8,11*b*(11)-triazabeno[*c*]fluorene **14.** Compound **14** was prepared using the above described method from compound **10** (0.25 g, 0.66 mmol) in sulfolane (1 ml) after 30 min to obtain grey powder (0.19 g, 82%). mp > 270 °C; UV (EtOH) λ_{max}/nm = 352, 305; IR (diamond): ν/cm⁻¹ = 3066, 1712, 1630, 1618, 1517; ¹H NMR (DMSO-*d*₆, 300 MHz): δ/ppm = a) 9.73 (d, 1H, *J* = 9.3 Hz, H_{arom}), 9.04 (dd, 2H, *J*₁ = 9.2 Hz, *J*₂ = 2.6 Hz, H_{arom}), 8.69 (dd, 1H, *J*₁ = 9.3 Hz, *J*₂ = 2.6 Hz, H_{arom}), 8.64 (d, 1H, *J* = 2.1 Hz, H_{arom}), 8.26 (d, 1H, *J* = 9.2 Hz, H_{arom}), 7.79 (d, 1H, *J* = 9.6 Hz, H_{fluorene}); b) 9.37 (d, 1H, *J* = 1.9 Hz, H_{arom}), 8.95 (d, 1H, *J* = 9.2 Hz, H_{arom}), 8.81 (d, 1H, *J* = 1.9 Hz, H_{arom}), 8.73 (d, 1H, *J* = 2.0 Hz, H_{arom}), 8.48 (dd, 1H, *J*₁ = 9.2 Hz, *J*₂ = 2.5 Hz, H_{arom}), 8.30 (Abq, *J* = 9.5 Hz, H_{fluorene}), 7.86 (d, 1H,

Table 5
Flow cytometric analysis of the MiaPaCa-2 and SW620 cell cycle progression upon treatment with compound **28**.

Compound 28	MiaPaCa-2				SW620			
	Cell percentage (% ± standard deviation)				Cell percentage (% ± standard deviation)			
Treatment	sub-G1	G1	S	G2/M	sub-G1	G1	S	G2/M
Control 24h	48.7 ± 0.7	51.2 ± 2.7	29.2 ± 4.2	19.5 ± 3.9	48.7 ± 0.7	51.2 ± 2.7	29.2 ± 4.2	19.5 ± 3.9
1 μM 24h	57.8 ± 1.7*	41.6 ± 1.8*	37.4 ± 2.5*	21.3 ± 2.6	57.8 ± 1.7*	41.6 ± 1.8*	37.4 ± 2.5*	21.3 ± 2.6
5 μM 24h	53.4 ± 0.3*	22.4 ± 1*	59.3 ± 2.1*	18.3 ± 2.6	53.4 ± 0.3*	22.4 ± 1*	59.3 ± 2.1*	18.3 ± 2.6
10 μM 24h	50.2 ± 2.3	52.4 ± 1.9	29.3 ± 1.5	18.3 ± 1.9	50.2 ± 2.3	52.4 ± 1.9	29.3 ± 1.5	18.3 ± 1.9
Control 48h	46.8 ± 0.7	65.2 ± 1.9	20.5 ± 0.2	14.3 ± 1.8	46.8 ± 0.7	65.2 ± 1.9	20.5 ± 0.2	14.3 ± 1.8
1 μM 48h	33.8 ± 0.7*	42.4 ± 1.8*	34.6 ± 0.7*	23 ± 2.1*	33.8 ± 0.7*	42.4 ± 1.8*	34.6 ± 0.7*	23 ± 2.1*
5 μM 48h	56.6 ± 2.5*	42.4 ± 1.5*	36.8 ± 1.4*	20.8 ± 1.9*	56.6 ± 2.5*	42.4 ± 1.5*	36.8 ± 1.4*	20.8 ± 1.9*
10 μM 48h	39.3 ± 0.9*	26.1 ± 5.1*	56.9 ± 4.8*	16.9 ± 2.4	39.3 ± 0.9*	26.1 ± 5.1*	56.9 ± 4.8*	16.9 ± 2.4
SW620								
Control 24h	18 ± 1	29.3 ± 1.5	48.4 ± 1.4	22.3 ± 2.9	18 ± 1	29.3 ± 1.5	48.4 ± 1.4	22.3 ± 2.9
1 μM 24h	14.3 ± 1.1*	54.3 ± 2.5*	27.2 ± 0.4*	18.5 ± 2.5	14.3 ± 1.1*	54.3 ± 2.5*	27.2 ± 0.4*	18.5 ± 2.5
5 μM 24h	24.4 ± 0.5*	86.1 ± 1.7*	11.8 ± 1.5*	2.1 ± 0.3*	24.4 ± 0.5*	86.1 ± 1.7*	11.8 ± 1.5*	2.1 ± 0.3*
10 μM 24h	20.1 ± 1.1	33.7 ± 2.1*	47.3 ± 2.8	19.2 ± 0.9	20.1 ± 1.1	33.7 ± 2.1*	47.3 ± 2.8	19.2 ± 0.9
Control 48h	29.1 ± 1.1	52.7 ± 0.9	31.9 ± 1	16.1 ± 0.9	29.1 ± 1.1	52.7 ± 0.9	31.9 ± 1	16.1 ± 0.9
1 μM 48h	25.4 ± 0.9*	35.1 ± 2.6*	45.4 ± 3.1*	19.4 ± 0.7*	25.4 ± 0.9*	35.1 ± 2.6*	45.4 ± 3.1*	19.4 ± 0.7*
5 μM 48h	47.6 ± 0.6*	90.9 ± 3*	7.5 ± 2.5*	1.5 ± 0.5*	47.6 ± 0.6*	90.9 ± 3*	7.5 ± 2.5*	1.5 ± 0.5*
10 μM 48h	40.6 ± 1.1*	39.9 ± 2.4*	41.8 ± 2.6*	18.2 ± 1.2	40.6 ± 1.1*	39.9 ± 2.4*	41.8 ± 2.6*	18.2 ± 1.2

(*) Statistically significant at *p* < 0.05.

Table 6
Flow cytometric analysis of the SK-BR-3 cell cycle progression upon treatment with compound **18**.

Compound 18	SK-BR-3			
	Cell percentage (% ± standard deviation)			
Treatment	sub-G1	G1	S	G2/M
Control 24h	39 ± 1.1	39.5 ± 1.1	39.9 ± 1.5	20.6 ± 2.1
5 μM 24h	35.7 ± 1.6*	47.1 ± 0.8*	35.1 ± 1.5*	17.7 ± 1.9
10 μM 24h	45.8 ± 1.7*	39.4 ± 4.7	34.5 ± 2.4*	26.1 ± 2.2*
50 μM 24h	50.2 ± 0.8*	33.2 ± 3.7	48.1 ± 3.1*	18.7 ± 0.9
Control 48h	2.1 ± 0.2	24.7 ± 1.9	40.6 ± 4.9	34.7 ± 3.3
5 μM 48h	1.9 ± 0.3	24.4 ± 3.5	59.8 ± 4.4*	15.8 ± 3.3*
10 μM 48h	5.5 ± 0.8*	20.9 ± 1.9	64.2 ± 2.1*	14.8 ± 0.2*
50 μM 48h	3.1 ± 0.1*	19.9 ± 0.8*	47.6 ± 1.5*	32.5 ± 1.1*

(*) Statistically significant at *p* < 0.05.

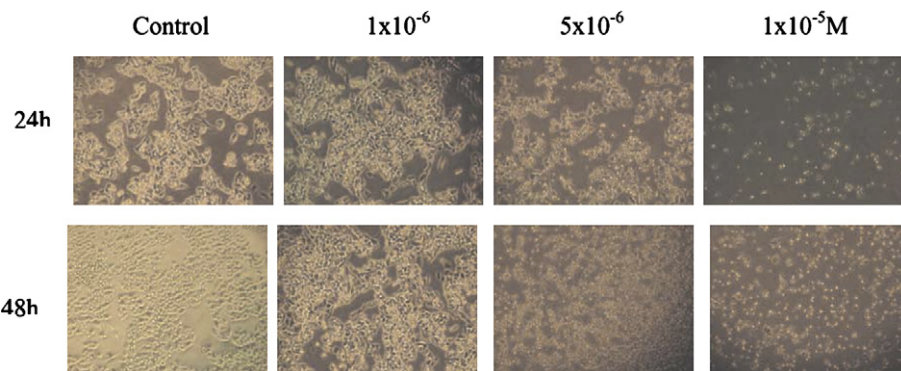


Fig. 5. MiaPaCa-2 cells treated with compound **28** for 24 and 48 h.

$J = 9.6$ Hz, $H_{\text{arom.}}$); ^{13}C NMR (DMSO- d_6 , 75 MHz): $\delta/\text{ppm} = 150.2, 148.1, 143.9, 138.1, 133.6, 125.8, 125.5, 124.9, 124.1, 123.5, 119.4, 118.0, 116.6, 113.8$; Anal. ($\text{C}_{14}\text{H}_7\text{N}_4\text{O}_2\text{Br}$) Calcd.: C, 49.0; H, 2.1; N, 16.3; Found: C, 49.3; H, 2.2; N, 16.2.

4.1.2.3. *1,7,8,11b(11)-Tetraazabenzoc[*c*]fluorene 15*. Compound **15** was prepared using the above described method from compound **11** (0.50 g, 2.05 mmol) in sulfolane (1.5 ml) after 45 min to obtain dark yellow powder (0.15 g, 24%). mp 186–187 °C; UV (EtOH) $\lambda_{\text{max}}/\text{nm} = 369, 351, 335, 324$; IR (diamond): $\nu/\text{cm}^{-1} = 3078, 1640, 1611$ and 1555; ^1H NMR (DMSO- d_6 , 600 MHz): $\delta/\text{ppm} = \text{a) } 9.33$ (dd, 1H, $J_1 = 8.1$ Hz, $J_2 = 1.7$ Hz, $H_{\text{arom.}}$), 8.93 (dd, 1H, $J_1 = 4.6$ Hz, $J_2 = 1.6$ Hz, $H_{\text{arom.}}$), 8.73 (dd, 1H, $J_1 = 4.7$ Hz, $J_2 = 1.6$ Hz, $H_{\text{arom.}}$), 8.58 (dd, 1H, $J_1 = 7.8$ Hz, $J_2 = 1.7$ Hz, $H_{\text{arom.}}$), 8.12 (d, 1H, $J = 9.5$ Hz, H_{fluorene}), 7.83 (d, 1H, $J = 9.5$ Hz, H_{fluorene}), 7.73–7.69 (m, 1H, $H_{\text{arom.}}$), 7.75 (dd, 1H, $J_1 = 8.1$ Hz, $J_2 = 4.7$ Hz, $H_{\text{arom.}}$); b) 8.93 (dd, 1H, $J_1 = 4.6$ Hz, $J_2 = 1.6$ Hz, $H_{\text{arom.}}$), 8.68 (dd, 1H, $J_1 = 4.4$ Hz, $J_2 = 1.3$ Hz, $H_{\text{arom.}}$), 8.51 (dd, 1H, $J_1 = 7.8$ Hz, $J_2 = 1.8$ Hz, $H_{\text{arom.}}$), 8.33 (dd, 1H, $J_1 = 8.1$ Hz, $J_2 = 1.5$ Hz, $H_{\text{arom.}}$), 8.05 (d, 1H, $J = 9.5$ Hz, H_{fluorene}), 7.74 (d, 1H, $J = 9.5$ Hz, H_{fluorene}), 7.72–7.67 (m, 1H, $H_{\text{arom.}}$), 7.61 (dd, 1H, $J_1 = 8.2$ Hz, $J_2 = 4.7$ Hz, $H_{\text{arom.}}$); ^{13}C NMR (DMSO- d_6 , 150 MHz): $\delta/\text{ppm} = \text{a) } 156.2, 150.2, 149.8, 147.5, 146.6, 138.7, 136.7, 132.3, 127.6, 121.7, 121.2, 118.6, 118.5$; b) 154.2, 150.0, 149.2, 146.2, 144.3, 138.9, 132.1, 124.9, 123.0, 121.6, 119.0, 118.5, 118.1; Anal. ($\text{C}_{13}\text{H}_8\text{N}_4$) Calcd.: C, 70.9; H, 3.7; N, 25.4; Found: C, 71.1; H, 3.8; N, 25.6.

4.1.3. General method for the synthesis of 8-*N*-methyl-triaza-benzoc[*c*]fluorene iodide derivatives (**16–17**)

Equimolar amounts of triaza-benzoc[*c*]fluorenes **12–13** and methyl-iodide in absolute ethanol (10 ml) were stirred at room temperature for 48 h. The solution was concentrated and obtained

product was filtered off and recrystallized from ethanol or water to obtain *N*-methyl-triaza-benzoc[*c*]fluorene iodides.

4.1.3.1. *8-N-Methyl-7,8,11b(11)-triazabenzoc[*c*]fluorene iodide 16*. Compound **16** was prepared using the above described method from compound **12** (0.04 g, 0.18 mmol) and methyl-iodide (12 μL , 0.18 mmol) to obtain yellow powder (0.02 g, 28%). mp >270 °C; UV (EtOH) $\lambda_{\text{max}}/\text{nm} = 361, 344, 328, 225$; IR (diamond): $\nu/\text{cm}^{-1} = 2916, 1661, 1619, 1552, 1433$; ^1H NMR (DMSO- d_6 , 600 MHz): $\delta/\text{ppm} = 10.67$ (d, 1H, $J = 8.7$ Hz, $H_{\text{arom.}}$), 9.00 (dd, 1H, $J_1 = 4.6$ Hz, $J_2 = 1.4$ Hz, $H_{\text{arom.}}$), 8.91 (d, 1H, $J = 9.7$ Hz, H_{fluorene}), 8.80 (dd, 1H, $J_1 = 7.5$ Hz, $J_2 = 1.4$ Hz, $H_{\text{arom.}}$), 8.43 (d, 1H, $J = 9.7$ Hz, H_{fluorene}), 8.41 (dd, 1H, $J_1 = 8.2$ Hz, $J_2 = 1.8$ Hz, $H_{\text{arom.}}$), 8.24 (t, 1H, $J = 8.1$ Hz, $H_{\text{arom.}}$), 8.05 (dd, 1H, $J_1 = 8.4$ Hz, $J_2 = 4.8$ Hz), 7.95 (t, 1H, $J = 7.7$ Hz, $H_{\text{arom.}}$), 4.31 (s, 3H, CH_3); ^{13}C NMR (DMSO- d_6 , 150 MHz): $\delta/\text{ppm} = 146.4, 143.5, 141.6, 140.9, 133.6, 132.7, 130.4, 127.7, 126.5, 123.5, 123.5, 122.5, 118.2, 109.2$; Anal. ($\text{C}_{15}\text{H}_{13}\text{N}_3\text{I}$) Calcd.: C, 49.9; H, 3.4; N, 11.7; Found: C, 50.1; H, 3.2; N, 11.8.

4.1.3.2. *3-Nitro-8-N-methyl-7,8,11b(11)-triazabenzoc[*c*]fluorene iodide 17*. Compound **17** was prepared using the above described method from compound **13** (0.10 g, 0.38 mmol) and methyl-iodide (24 μL , 0.38 mmol) to obtain yellow powder (0.02 g, 15%). mp >270 °C; UV (EtOH) $\lambda_{\text{max}}/\text{nm} = 383, 365, 297, 263, 225$; IR (diamond): $\nu/\text{cm}^{-1} = 3044, 2765, 1656, 1611, 1544$; ^1H NMR (DMSO- d_6 , 600 MHz): $\delta/\text{ppm} = \text{a) } 9.21$ (d, 1H, $J = 8.5$ Hz, $H_{\text{arom.}}$), 9.32 (d, 1H, $J = 2.6$ Hz, $H_{\text{arom.}}$), 9.21 (d, 1H, $J = 9.4$ Hz, $H_{\text{arom.}}$), 9.18 (d, 1H, $J = 6.1$ Hz, $H_{\text{arom.}}$), 8.76 (d, 1H, $J = 9.5$ Hz, $H_{\text{arom.}}$), 8.70 (dd, 1H, $J_1 = 9.3$ Hz, $J_2 = 2.7$ Hz, $H_{\text{arom.}}$), 8.23 (d, 1H, $J = 9.5$ Hz, $H_{\text{arom.}}$), 8.11 (dd, 1H, $J_1 = 8.4$ Hz, $J_2 = 6.2$ Hz, $H_{\text{arom.}}$), 4.33 (s, 3H, CH_3); b) 9.64 (d, 1H, $J = 8.9$ Hz, $H_{\text{arom.}}$), 9.42 (d, 1H, $J = 2.3$ Hz, $H_{\text{arom.}}$), 9.37 (d, 1H, $J = 9.1$ Hz, $H_{\text{arom.}}$), 9.12 (dd,

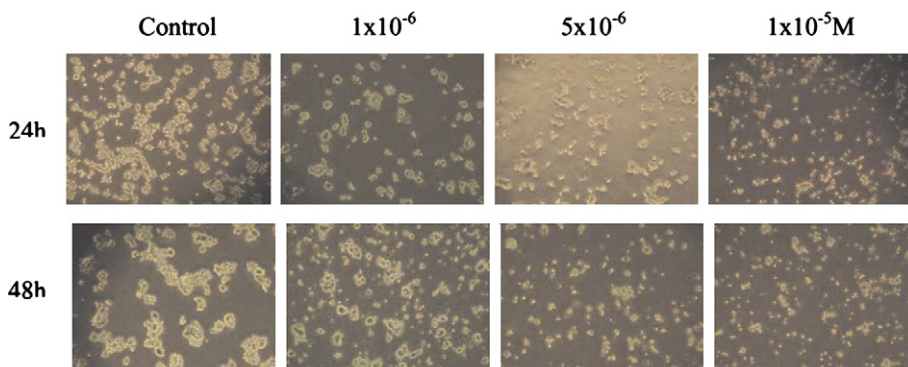


Fig. 6. SW620 cells treated with compound **28** for 24 and 48 h.

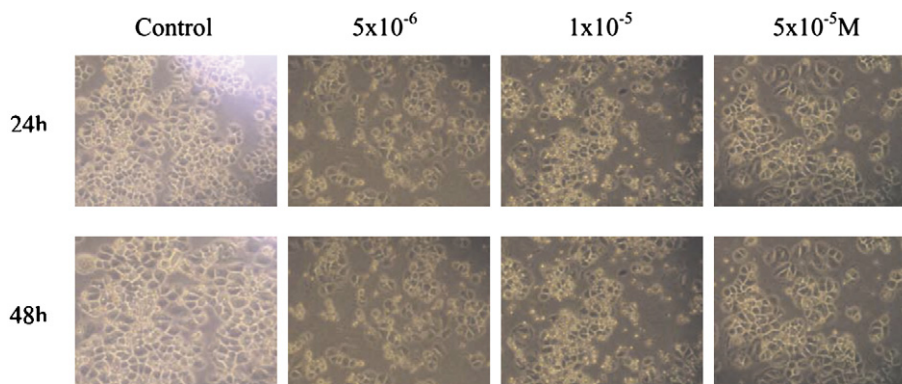


Fig. 7. SK-BR-3 cells treated with compound **18** for 24 and 48 h.

^1H , $J_1 = 4.9$ Hz, $J_2 = 2.4$ Hz, $H_{\text{arom.}}$), 9.04 (d, 1H, $J = 4.6$ Hz, $H_{\text{arom.}}$), 9.00 (d, 1H, $J = 9.2$ Hz, $H_{\text{arom.}}$), 8.80 (dd, 1H, $J_1 = 9.3$ Hz, $J_2 = 2.5$ Hz, $H_{\text{arom.}}$), 8.68 (d, 1H, $J = 9.5$ Hz, $H_{\text{arom.}}$), 4.27 (s, 3H, CH_3); ^{13}C NMR (DMSO- d_6 , 150 MHz): $\delta/\text{ppm} = 151.9, 149.7, 145.2, 141.9, 138.6, 137.6, 131.8, 128.4, 126.7, 126.2, 124.3, 118.8, 118.6, 42.2$; Anal. ($\text{C}_{15}\text{H}_{11}\text{N}_4\text{O}_2$) Calcd.: C, 44.4; H, 2.7; N, 13.8; Found: C, 44.5; H, 2.8; N, 13.5.

4.1.4. General method for the synthesis of 3-amino-triaza-benzo[*c*]fluorene derivatives (**18–19**)

Corresponding 3-nitro-triaza-benzo[*c*]fluorene derivatives **13–14** and solution of $\text{SnCl}_2 \times 2\text{H}_2\text{O}$ in H_2O and concentrated HCl were refluxed for 30 min. After cooling, the reaction mixture was evaporated under vacuum and dissolved in water (50 ml). The resulting solution was treated with 20% NaOH to pH 14. The resulting product was filtered off and washed with water to obtain 3-amino-triaza-benzo[*c*]fluorenes.

4.1.4.1. 3-Amino-7,8,11b(11)-triazabeno[*c*]fluorene **18.** Compound **18** was prepared using the above described method from compound **13** (0.13 g, 0.49 mmol), $\text{SnCl}_2 \times 2\text{H}_2\text{O}$ (0.92 g, 4.00 mmol), HCl_{conc} (1.7 ml) and H_2O (1.7 ml) to yellow powder (0.08 g, 69%). mp 206–208 °C; UV (EtOH) $\lambda_{\text{max}}/\text{nm} = 349, 335, 270, 245$; IR (diamond): $\nu/\text{cm}^{-1} = 3224, 3016, 1705, 1634, 1520$; ^1H NMR (DMSO- d_6 , 300 MHz): $\delta/\text{ppm} =$ a) 9.02 (dd, 1H, $J_1 = 8.3$ Hz, $J_2 = 1.2$ Hz, $H_{\text{arom.}}$), 8.64 (dd, 1H, $J_1 = 4.6$ Hz, $J_2 = 1.2$ Hz, $H_{\text{arom.}}$), 8.49 (d, 1H, $J = 8.9$ Hz, $H_{\text{arom.}}$), 7.85 (d, 1H, $J = 9.5$ Hz, $H_{\text{arom.}}$), 7.58 (d, 1H, $J = 9.5$ Hz, $H_{\text{arom.}}$), 7.42 (dd, 1H, $J_1 = 8.3$ Hz, $J_2 = 4.6$ Hz, $H_{\text{arom.}}$), 7.16 (dd, 1H, $J_1 = 8.9$ Hz, $J_2 = 2.6$ Hz, $H_{\text{arom.}}$), 7.10 (d, 1H, $J = 2.5$ Hz, $H_{\text{arom.}}$); b) 9.49 (d, 1H, $J = 8.7$ Hz, $H_{\text{arom.}}$), 8.57 (dd, 1H, $J_1 = 4.7$ Hz, $J_2 = 1.4$ Hz, $H_{\text{arom.}}$), 8.26 (dd, 1H, $J_1 = 8.2$ Hz, $J_2 = 1.5$ Hz, $H_{\text{arom.}}$), 7.82 (d, 1H, $J = 9.4$ Hz, $H_{\text{arom.}}$), 7.56 (d, 1H, $J = 9.5$ Hz, $H_{\text{arom.}}$), 7.52 (dd, 1H, $J_1 = 8.3$ Hz, $J_2 = 1.4$ Hz, $H_{\text{arom.}}$), 7.14 (dd, 1H, $J_1 = 8.8$ Hz, $J_2 = 2.6$ Hz, $H_{\text{arom.}}$), 7.09 (d, 1H, $J = 2.6$ Hz, $H_{\text{arom.}}$); ^{13}C NMR (DMSO- d_6 , 75 MHz): a) 148.6, 146.7, 146.3, 136.7, 133.4, 127.4, 126.5, 124.7, 123.0, 120.2, 119.7, 118.7, 118.0, 117.0; b) 156.1, 147.5, 146.6, 145.1, 142.8, 133.3, 126.1, 124.4, 122.7, 119.9, 118.7, 118.4, 117.2, 116.9; Anal. ($\text{C}_{14}\text{H}_{10}\text{N}_4$) Calcd.: C, 71.8; H, 4.3; N, 23.9; Found: C, 71.9; H, 4.5; N, 24.1.

4.1.4.2. 3-Amino-10-bromo-7,8,11b(11)-triazabeno[*c*]fluorene **19**.

Compound **19** was prepared using the above described method from compound **14** (0.18 g, 0.53 mmol), $\text{SnCl}_2 \times 2\text{H}_2\text{O}$ (0.98 g, 4.34 mmol), HCl_{conc} (1.8 ml) and H_2O (1.8 ml) to obtain yellow powder (0.13 g, 82%). mp 252–254 °C; UV (EtOH) $\lambda_{\text{max}}/\text{nm} = 351, 339, 274, 249$; IR (diamond): $\nu/\text{cm}^{-1} = 3222, 3067, 1722, 1620, 1571$; ^1H NMR (DMSO- d_6 , 300 MHz): $\delta/\text{ppm} =$ a) 9.26 (d, 1H, $J = 8.9$ Hz, $H_{\text{arom.}}$), 8.67 (d, 1H, $J = 2.0$ Hz, $H_{\text{arom.}}$), 8.46 (d, 1H, $J = 8.7$ Hz, $H_{\text{arom.}}$),

7.85 (d, 1H, $J = 9.5$ Hz, $H_{\text{arom.}}$), 7.54 (d, 1H, $J = 9.5$ Hz, $H_{\text{arom.}}$), 7.17–7.12 (m, 2H, $H_{\text{arom.}}$), 5.57 (brs, 3H, NH_2); b) 9.20 (d, 1H, $J = 2.0$ Hz, $H_{\text{arom.}}$), 8.57 (d, 1H, $J = 2.1$ Hz, $H_{\text{arom.}}$), 8.45 (d, 1H, $J = 9.2$ Hz, $H_{\text{arom.}}$), 7.84 (d, 1H, $J = 9.6$ Hz, $H_{\text{arom.}}$), 7.47 (d, 1H, $J = 9.6$ Hz, $H_{\text{arom.}}$), 7.08–7.05 (m, 2H, $H_{\text{arom.}}$), 5.55 (brs, 3H, NH_2); ^{13}C NMR (DMSO- d_6 , 75 MHz): a) 149.5, 147.0, 142.7, 137.9, 134.0, 126.0, 124.7, 124.5, 118.6, 117.3, 116.7, 116.5, 112.1, 111.2; b) 154.6, 148.7, 146.9, 146.7, 137.9, 134.3, 129.3, 125.6, 123.7, 118.9, 117.8, 116.9, 115.2, 111.8; Anal. ($\text{C}_{14}\text{H}_9\text{N}_4\text{Br}$) Calcd.: C, 53.8; H, 2.9; N, 17.9; Found: C, 53.9; H, 3.1; N, 18.0.

4.1.5. General method for the synthesis of 3-amino-triaza-benzo[*c*]fluorene hydrochlorides (**20–21**)

A stirred suspension of compounds **18–19** in absolute ethanol (15 mL) was saturated with $\text{HCl}_{(\text{g})}$. After 24 h of stirring, small amount of diethylether was added, resulting product was filtered off and washed with diethylether to obtain 3-amino-triaza-benzo[*c*]fluorene hydrochlorides.

4.1.5.1. 3-Amino-7,8,11b(11)-triazabeno[*c*]fluorene hydrochloride **20.** Compound **20** was prepared using the above described method from compound **18** (0.06 g, 0.26 mmol) to obtain white powder (0.04 g, 52%). mp > 270 °C; UV (EtOH) $\lambda_{\text{max}}/\text{nm} = 347, 333, 270$ and 245; IR (diamond): $\nu/\text{cm}^{-1} = 3266, 3145, 1744, 1620, 1613, 1509$; ^1H NMR (DMSO- d_6 , 300 MHz): $\delta/\text{ppm} =$ a) 9.80 (d, 1H, $J = 9.1$ Hz, $H_{\text{arom.}}$), 8.88 (d, 1H, $J = 9.7$ Hz, $H_{\text{arom.}}$), 8.76 (dd, 1H, $J_1 = 4.7$ Hz, $J_2 = 1.4$ Hz, $H_{\text{arom.}}$), 8.44 (dd, 1H, $J_1 = 9.0$ Hz, $J_2 = 1.5$ Hz, $H_{\text{arom.}}$), 8.41 (d, 1H, $J = 9.7$ Hz, $H_{\text{arom.}}$), 7.89 (d, 1H, $J = 9.5$ Hz, $H_{\text{arom.}}$), 7.81–7.76 (m, 2H, $H_{\text{arom.}}$), 6.54 (brs, 3H, NH_3^+); b) 9.52 (d, 1H, $J = 8.5$ Hz, $H_{\text{arom.}}$), 8.84 (d, 1H, $J = 4.5$ Hz, $H_{\text{arom.}}$), 8.76 (dd, 1H, $J_1 = 4.7$ Hz, $J_2 = 1.3$ Hz, $H_{\text{arom.}}$), 8.37 (d, 1H, $J = 9.7$ Hz, $H_{\text{arom.}}$), 7.86 (d, 1H, $J = 9.5$ Hz, $H_{\text{arom.}}$), 7.80–7.71 (m, 3H, $H_{\text{arom.}}$), 6.53 (brs, 3H, NH_3^+); ^{13}C NMR (DMSO- d_6 , 75 MHz): a) 149.1, 145.2, 144.9, 137.5, 137.1, 131.9, 130.0, 127.7, 124.8, 124.4, 122.5, 119.1, 118.3, 115.2; b) 148.2, 143.9, 143.8, 137.0, 136.8, 129.2, 125.9, 125.1, 124.8, 124.1, 121.1, 118.8, 118.1, 114.8; Anal. ($\text{C}_{14}\text{H}_{11}\text{N}_4\text{Cl}$) Calcd.: C, 62.1; H, 4.1; N, 20.7; Found: C, 62.3; H, 4.3; N, 20.9.

4.1.5.2. 3-Amino-10-bromo-7,8,11b(11)-triazabeno[*c*]fluorene hydrochloride **21.** Compound **21** was prepared using the above described method from compound **19** (0.07 g, 0.22 mmol) to obtain yellow powder (0.03 g, 41%). mp > 270 °C; UV (EtOH) $\lambda_{\text{max}}/\text{nm} = 354, 340, 273, 249$; IR (diamond): $\nu/\text{cm}^{-1} = 3268, 3209, 3089, 1742, 1645, 1580$; ^1H NMR (DMSO- d_6 , 300 MHz): $\delta/\text{ppm} =$ 9.58 (d, 1H, $J = 9.1$ Hz, $H_{\text{arom.}}$), 8.80 (d, 1H, $J = 1.5$ Hz, $H_{\text{arom.}}$), 8.69 (d, 1H, $J = 1.9$ Hz, $H_{\text{arom.}}$), 8.24 (d, 1H, $J = 9.6$ Hz, $H_{\text{arom.}}$), 8.01 (s, 1H, $H_{\text{arom.}}$), 7.86 (dd, 1H, $J_1 = 8.9$ Hz, $J_2 = 1.9$ Hz, $H_{\text{arom.}}$), 7.78 (d, 1H, $J = 9.5$ Hz,

H_{arom.}), 7.50 (brs, 3H, NH₃⁺); b) 9.39 (d, 1H, *J* = 1.6 Hz, H_{arom.}), 8.87 (d, 1H, *J* = 8.9 Hz, H_{arom.}), 8.60 (d, 1H, *J* = 1.9 Hz, H_{arom.}), 8.21 (d, 1H, *J* = 9.6 Hz, H_{arom.}), 8.00 (s, 1H, H_{arom.}), 7.85 (dd, 1H, *J*₁ = 8.9 Hz, *J*₂ = 1.9 Hz, H_{arom.}), 7.78 (d, 1H, *J* = 9.6 Hz, H_{arom.}), 7.51 (brs, 3H, NH₃⁺); ¹³C NMR (DMSO-*d*₆, 75 MHz): a) 148.4, 147.4, 143.1, 134.4, 125.4, 124.5, 124.3, 123.5, 123.1, 118.1, 117.7, 116.9, 115.6, 113.8; b) 147.6, 144.6, 133.3, 125.1, 124.9, 123.8, 123.4, 118.8, 117.9, 117.6, 116.5, 115.7, 113.5, 113.2; Anal. (C₁₄H₁₀N₄ClBr) Calcd.: C, 48.1; H, 2.9; N, 16.0; Found: C, 48.3; H, 3.0; N, 16.3.

4.1.6. General method for the synthesis of cyano-triaza-benzo[c]fluorenes (26–27)

Ethanol solution (400 ml) of compounds **24–25** was irradiated for 11 h at room temperature with 400 W high-pressure mercury lamp using the Pyrex filter. The air was bubbled through the solution, and the latter was concentrated. The obtained product was filtered off to produce cyano-triaza-benzo[c]fluorenes.

4.1.6.1. 2-Cyano-7,8,11b-triazabenzoc[fluorene 26. Compound **26** was prepared using the above described method from compound **24** (0.30 g, 1.22 mmol) to obtain yellow powder (0.17 g, 57%). mp 252–254 °C; UV (EtOH) λ_{max}/nm = 381, 362, 345, 234; IR (diamond): ν/cm⁻¹ = 1614, 1640, 1966, 2224, 3067; ¹H NMR (DMSO-*d*₆, 300 MHz): δ/ppm = 10.06 (s, 1H, NH), 8.10 (dd, 1H, *J*₁ = 4.6 Hz, *J*₂ = 1.2 Hz, H_{arom.}), 8.38 (dd, 1H, *J*₁ = 8.2 Hz, *J*₂ = 1.0 Hz, H_{arom.}), 8.23 (d, 1H, *J* = 8.1 Hz, H_{arom.}), 8.08 (d, 1H, *J* = 9.6 Hz, H_{arom.}), 7.98 (d, 1H, *J* = 8.2 Hz, H_{arom.}), 7.82 (d, 1H, *J* = 9.6 Hz, H_{arom.}), 7.64 (Abq, 1H, *J*₁ = 8.2 Hz, *J*₂ = 4.8 Hz, H_{arom.}); ¹³C NMR (DMSO-*d*₆, 75 MHz): 149.6, 145.5, 144.1, 137.1, 134.5, 132.3, 130.7, 129.5, 128.4, 127.9, 126.4, 121.2, 120.9, 118.9, 112.3; Anal. (C₁₅H₈N₄) Calcd.: C, 73.8; H 3.3; N, 22.9; Found: C, 73.9; H, 3.1; N, 23.1.

4.1.6.2. 10-Bromo-2-cyano-7,8,11b-triazabenzoc[fluorene 27. Compound **27** was prepared using the above described method from compound **25** (0.14 g, 0.46 mmol) to obtain yellow powder (0.06 g, 42%). mp > 270 °C; UV (EtOH) λ_{max}/nm = 382, 361, 345, 235; IR (diamond): ν/cm⁻¹ = 1536, 1570, 1625, 2226, 3076; ¹H NMR (DMSO-*d*₆, 300 MHz): δ/ppm = 8.41 (d, 1H, *J* = 2.1 Hz, H_{arom.}), 8.23 (d, 1H, *J* = 2.0 Hz, H_{arom.}), 7.87 (d, 4H, *J* = 8.4 Hz, H_{arom.}), 7.83 (d, 1H, *J* = 16.6 Hz, H_{arom.}), 7.38 (d, 1H, *J* = 16.5 Hz, H_{arom.}); ¹³C NMR (DMSO-*d*₆, 75 MHz): δ/ppm = not soluble enough; Anal. (C₁₅H₇N₄Br) Calcd.: C, 55.8; H, 2.2; N, 17.3; Found: C, 55.9; H, 2.4; N, 17.2.

4.1.7. General method for the synthesis of 2-imidazolynyl-triaza-benzo[c]fluorene hydrochlorides (28–29)

A stirred suspension of corresponding cyano-triaza-benzo[c]fluorenes **26–27** in absolute ethanol was cooled in an ice-salt bath and was saturated with HCl gas. The flask was then tightly stoppered, and the mixture was maintained at room temperature until the nitrile band disappeared (monitored by the IR analysis at 2200 cm⁻¹). The reaction mixture was purged with N₂ gas and diluted with diethylether. The crude imidate was filtered off and was immediately suspended in absolute ethanol. Ethylenediamine was added and the mixture was stirred at reflux for 24 h. The crude product was then filtered off, washed with diethylether to give white powder, which was suspended in absolute ethanol and again saturated with HCl (g). Reaction mixture was stirred at room temperature for 24 h. Crude product was filtered off and washed with small amount of diethylether to give corresponding 2-imidazolynyl-triaza-benzo[c]fluorene hydrochlorides.

4.1.7.1. 2-(2-Imidazolynyl)-7,8,11b-triazabenzoc[fluorene hydrochloride 28. Compound **28** was prepared using the above described method from compound **26** (0.20 g, 0.82 mmol) and ethylenediamine (0.16 ml, 2.32 mmol) to obtain light green powder (0.06 g,

32%). mp > 270 °C; UV (EtOH) λ_{max}/nm = 366, 350, 237; IR (diamond): ν/cm⁻¹ = 1603, 1620, 1713, 3013, 3295; ¹H NMR (DMSO-*d*₆, 600 MHz): δ/ppm = 11.01 (s, 2H, NH), 10.25 (s, 1H, H_{arom.}), 8.75 (dd, 1H, *J*₁ = 4.7 Hz, *J*₂ = 1.4 Hz, H_{arom.}), 8.44 (dd, 1H, *J*₁ = 8.1 Hz, *J*₂ = 1.4 Hz, H_{arom.}), 8.35 (d, 1H, *J* = 8.2 Hz, H_{arom.}), 8.20 (d, 1H, *J* = 9.5 Hz, H_{arom.}), 8.09 (dd, 1H, *J*₁ = 8.2 Hz, *J*₂ = 1.6 Hz, H_{arom.}), 7.92 (d, 1H, *J* = 9.6 Hz, H_{arom.}), 7.71 (dd, 1H, *J*₁ = 8.2 Hz, *J*₂ = 4.7 Hz, H_{arom.}), 4.15 (s, 4H, CH₂); ¹³C NMR (DMSO-*d*₆, 75 MHz): δ/ppm = 165.9, 147.4, 145.1, 141.1, 135.4, 134.1, 133.4, 130.7, 128.0, 127.3, 125.1, 124.2, 121.1, 120.2, 117.6, 45.3 (2C); Anal. (C₁₇H₁₄N₅Cl) Calcd.: C, 63.1; H, 4.4; N, 21.6; Found: C, 63.2; H, 4.2; N, 21.4.

4.1.7.2. 10-Bromo-2-(2-imidazolynyl)-7,8,11b-triazabenzoc[fluorene 29. Compound **28** was prepared using the above described method from compound **27** (0.11 g, 0.33 mmol) and ethylenediamine (0.08 ml, 1.16 mmol) to obtain light green powder (0.07 g, 65%). mp > 270 °C; IR (diamond): ν/cm⁻¹ = 1598, 1614, 1723, 2988, 3383; UV (EtOH) λ_{max}/nm = 355, 247; ¹H NMR (DMSO-*d*₆, 600 MHz): δ/ppm = 11.00 (s, 2H, NH), 10.05 (s, 1H, H_{arom.}), 8.74 (d, 1H, *J* = 1.0 Hz, H_{arom.}), 8.72 (d, 1H, *J* = 1.0 Hz, H_{arom.}), 8.34 (d, 1H, *J* = 4.1 Hz, H_{arom.}), 8.19 (d, 1H, *J* = 4.8 Hz, H_{arom.}), 8.08 (d, 1H, *J* = 4.1 Hz, H_{arom.}), 7.89 (d, 1H, *J* = 4.8 Hz, H_{arom.}), 4.12 (s, 4H, CH₂); ¹³C NMR (DMSO-*d*₆, 75 MHz): δ/ppm = 165.2, 148.5, 143.5, 143.5, 137.5, 133.5, 133.0, 129.9, 126.7, 125.6, 124.8, 120.2, 116.8, 115.8, 44.7; Anal. (C₁₇H₁₃N₅ClBr) Calcd.: C, 50.8; H, 3.2; N, 17.5; Found: C, 50.9; H, 3.4; N, 17.4.

4.2. Spectroscopy

The electronic absorption spectra were recorded on Varian Cary 50 and Varian Cary 100 Bio spectrometer, CD spectra on Jasco J815, in all cases using quartz cuvettes (1 cm). Fluorescence emission spectra were recorded on Varian Eclipse fluorimeter (quartz cuvettes, 1 cm) at 350–600 nm. The sample concentration in fluorescence measurements had an optical absorbance below 0.05 at the excitation wavelength. Under the experimental conditions used, the absorbance and fluorescence intensities of studied compounds were proportional to their concentrations, while none of studied compounds showed CD spectra. The measurements were performed in an aqueous buffer solution (pH = 7.0; sodium cacodylate buffer, *I* = 0.05 mol dm⁻³).

4.3. Interactions with DNA

The calf thymus DNA (ct-DNA) was purchased from Sigma–Aldrich, dissolved in sodium cacodylate buffer, *I* = 0.05 mol dm⁻³, pH = 7.0, additionally sonicated, filtered through 0.45 μm filter, and the concentration of the corresponding solution was determined spectroscopically as the concentration of phosphates [34]. The measurements were performed in an aqueous buffer solution (pH = 7.0; sodium cacodylate buffer, *I* = 0.05 mol dm⁻³). Spectroscopic titrations were performed by adding portions of polynucleotide solution into the solution of the studied compound. The stability constant (*K*_s) and [bound compound]/[polynucleotide phosphate] ratio (*n*) were calculated according to the Scatchard equation by non-linear least-square fitting giving excellent correlation coefficients (>0.999) for obtained values for *K*_s and *n*. Thermal denaturation curves for ct-DNA and its complexes with studied compounds were determined as previously described by following the absorption change at 260 nm as a function of temperature. The absorbance of the ligand was subtracted from every curve, and the absorbance scale was normalized. Obtained *T*_m values are the midpoints of the transition curves, determined from the maximum of the first derivative or graphically by a tangent method. Given Δ*T*_m values were calculated subtracting *T*_m of the free nucleic acid from *T*_m of complex. Every Δ*T*_m value here reported was the average of at least two measurements, the error in Δ*T*_m is ± 0.5 °C.

4.4. Cell culturing and cell morphology

The cell lines HeLa (cervical carcinoma), SW620 (colorectal adenocarcinoma, metastatic), MiaPaCa-2 (pancreatic carcinoma), MCF-7 (breast epithelial adenocarcinoma, metastatic), HEP-2 (epidermoid carcinoma, larynx), SK-BR-3 (breast adenocarcinoma, metastatic) and WI38 (normal diploid human fibroblasts) were cultured as monolayers and maintained in Dulbecco's modified Eagle medium (DMEM) supplemented with 10% foetal bovine serum (FBS), 2 mM L-glutamine, 100 U/ml penicillin and 100 µg/ml streptomycin in a humidified atmosphere with 5% CO₂ at 37 °C. The evaluation of cell morphology was performed under the light invert microscope Olympus (magnification 200×).

4.5. Antitumour activity assays

The panel of monolayer tumour cell lines was inoculated into standard 96-well microtiter plates on day 0, at 3000–6000 cells per well depending on the doubling time of the specific cell line. Test compounds and control compounds (cisplatin and 5-fluorouracil, 5-FU) were then added in five 10-fold dilutions (0.01–100 µM) followed by 72-h incubation. Cell viability was quantitatively determined using the 3-(4,5-dimethylthiazol-2-yl)-2,5-diphenyltetrazolium bromide (MTT) colorimetric assay. Experimentally obtained absorbances were transformed into cell percentage growth (PG) using the formulae proposed by NIH and described previously [35]. The IC₅₀ values for each compound were calculated from concentration–response curves using linear regression analysis by fitting the test concentrations that give PG values above and below the reference value. If, however, all of the tested concentrations produce PGs exceeding the respective reference level of effect (e.g. PG value of 50) for a given cell line, the highest tested concentration is assigned as the default value (in the screening data report, that default value is preceded by a ">" sign). Each test point was performed in quadruplicate in three individual experiments. The results were statistically analyzed (ANOVA, Tukey post-hoc test at *p* < 0.05). Finally, the effects of the tested substances were evaluated by plotting the mean percentage growth for each cell type in comparison to control on dose–response graphs.

4.6. Cell cycle analyses

A total of 3×10^4 cells/well were seeded in 6-well plates (Falcon, USA). After 24 h, MiaPaCa-2 and SW620 cells were treated with compound **28** at concentrations of 1, 5 and 10 µM. SK-BR-3 cells were treated with compound **18** at concentrations of 5, 10 and 50 µM. After 24 and 48 h, attached cells were trypsinized, combined with floating cells, washed with PBS and fixed with 70% ethanol. Immediately before the analysis, the cells were washed again with PBS and stained with 10 µg/mL of propidium iodide (PI) with the addition of 0.2 µg/mL of RNase A. Stained cells were then analysed with Becton Dickinson FACScalibur flow cytometer (10000 counts were measured). Each test point was performed in triplicate. The percentage of the cells in each cell cycle phase was deduced from obtained DNA histograms using WinMDI 2.9 and Cylchred software. Statistical analysis was performed in Microsoft Excel by using ANOVA at *p* < 0.05.

Acknowledgement

Support for this study by the Croatian Ministry of Science, Education and Sport is gratefully acknowledged (Grants number

125-0982464-1356, 098-0982914-2918, 335-0982464-2393, and 335-0000000-3532).

Appendix. Supplementary material

Supplementary data associated with this article can be found, in the online version, at doi:10.1016/j.ejmech.2011.03.062.

References

- [1] R.P. Kale, M.U. Shaikh, G.R. Jadhav, C.H. Gill, Tet. Lett. 50 (2009) 1780–1782.
- [2] R.B. Silverman, The Organic Chemistry of Drug Design and Drug Action, second ed. Elsevier Academic Press, 2004.
- [3] C. Temple Jr., J.D. Rose, R.N. Comber, G.A. Renner, J. Med. Chem. 30 (1987) 1746–1751.
- [4] G. Cristalli, S. Vittori, A. Eleuteri, M. Grifantini, R. Volpini, G. Lupidi, L. Capolongo Pesenti, J. Med. Chem. 34 (1991) 2226–2230.
- [5] G. Cristalli, S. Vittori, A. Eleuteri, R. Volpini, E. Camaioni, G. Lupidi, N. Mohmoud, F. Bevilacqua, G. Palu, J. Med. Chem. 38 (1995) 4019–4025.
- [6] D.J. Cundy, G. Holan, M. Otaegui, G.W. Simpson, Bioorg. Med. Chem. Lett. 7 (1997) 669–674.
- [7] H. Banie, A. Sinha, R.J. Thomas, J.C. Sircar, M.L. Richards, J. Med. Chem. 50 (2007) 5984–5993.
- [8] C. Temple, J. Med. Chem. 33 (1990) 656–661.
- [9] M. Mader, et al., Bioorg. Med. Chem. Lett. 18 (2008) 179–183.
- [10] L. Bukowski, R. Kalisz, Arch. Pharm. 9 (1991) 537–542.
- [11] D.M. Feng, J.M. Wai, S.D. Kuduk, C. Ng, K.L. Murphy, R.W. Ransom, D. Reiss, R.S.L. Chang, C.M. Harrell, T. MacNeil, C. Tang, T. Prueksaranont, R.M. Freidinger, D.J. Pettibone, M. Bocka, Bioorg. Med. Chem. Lett. 15 (2005) 2385–2388.
- [12] (a) Weier RM, Khanna IK, Stealey MA, Julien J. US Patent 5,262,426, (1993). (b) Weier RM, Khanna IK, Lentz K, Stealey MA, Julien J, US Patent 5,359,073, (1994).
- [13] S.S. Kulkarni, A.H. Newman, Bioorg. Med. Chem. Lett. 17 (2007) 2987–2991.
- [14] A. Cappelli, G. Pericot Mohr, G. Giuliani, S. Galeazzi, M. Anzini, L. Mennuni, F. Ferrari, F. Makovec, E.M. Kleinrath, T. Langer, M. Valoti, G. Giorgi, S. Vomero, J. Med. Chem. 49 (2006) 6451–6464.
- [15] V. Bavetsias, C. Sun, N. Bouloc, J. Reynisson, P. Workman, S. Linardopoulos, E. McDonald, Bioorg. Med. Chem. Lett. 17 (2007) 6567–6571.
- [16] W.J. Coates, B. Connolly, D. Dhanak, S.T. Flynn, A. Worby, J. Med. Chem. 36 (1993) 1387–1392.
- [17] C. Bailly, Curr. Med. Chem. 7 (2000) 39–58.
- [18] S.M. Nelson, L.R. Ferguson, A. Denny, Mutat. Res. 623 (2007) 24–40.
- [19] M. Demeunynck, C. Bailly, W.D. Wilson, DNA and RNA Binders. Wiley-VCH, Weinheim, 2002.
- [20] R. Martínez, L. Chacón-García, Curr. Med. Chem. 12 (2005) 127–151.
- [21] M.F. Brana, M. Cacho, A. Gradillas, B. de Pascual-Teresa, A. Ramos, Curr. Pharm. Design 7 (2005) 1745–1780.
- [22] M. Hranjec, M. Kralj, I. Piantanida, M. Sedić, L. Šuman, K. Pavelić, G. Karminski-Zamola, J. Med. Chem. 50 (2007) 5696–5711.
- [23] M. Hranjec, I. Piantanida, M. Kralj, L. Šuman, K. Pavelić, G. Karminski-Zamola, J. Med. Chem. 51 (2008) 4899–4910.
- [24] M. Sedić, M. Poznić, P. Gehrig, M. Scott, R. Schlapbach, M. Hranjec, G. Karminski-Zamola, K. Pavelić, S. Kraljević Pavelić, Mol. Cancer Ther. 7 (2009) 2121–2132.
- [25] J.A. Joule, K. Mills, Heterocyclic Chemistry, fourth ed. Blackwell Publishing, India, 2007.
- [26] M. Hranjec, G. Pavlović, M. Marinović, G. Karminski-Zamola, Struct. Chem. 19 (2008) 353–359.
- [27] P.K. Dubey, C.V. Ratnam, Ind. J. Chem. 18 (1979) 428–431.
- [28] J. Oszczapowicz, in: S. Patai, Z. Rappoport (Eds.), The Chemistry of Amidines and Imidates, vol. 2, John Wiley and Sons, London, New York, 1991.
- [29] T.A. Fairley, R.R. Tidwell, I. Donkor, N.A. Naiman, K.A. Ohemeng, R.J. Lombardy, J.A. Bentley, M. Cory, J. Med. Chem. 36 (1993) 1746.
- [30] a) G. Scatchard, Ann. N.Y. Acad. Sci. 51 (1949) 660–672; b) J.D. McGhee, P.H. von Hippel, J. Mol. Biol. 103 (1976) 679–684.
- [31] A. Rodger, B. Norden, in: Circular Dichroism and Linear Dichroism, Oxford University Press, New York, 1997.
- [32] M. Eriksson, B. Nordén, Methods Enzymol. 34 (2001) 68–98.
- [33] H.C. Becker, B. Norden, J. Am. Chem. Soc. 119 (1997) 5798–5803.
- [34] a) J.B. Chaires, N. Dattagupta, D.M. Crothers, Biochemistry 21 (1982) 3933–3940; b) I. Piantanida, B.S. Palm, P. Čudić, M. Žinić, H.J. Schneider, Tetrahedron 60 (2004) 6225–6231.
- [35] T. Gazivoda, M. Plevnik, J. Plavec, S. Kraljević, M. Kralj, K. Pavelić, J. Balzarini, E. De Clercq, M. Mintas, S. Raić-Malić, Bioorg. Med. Chem. 13 (2005) 131–139.